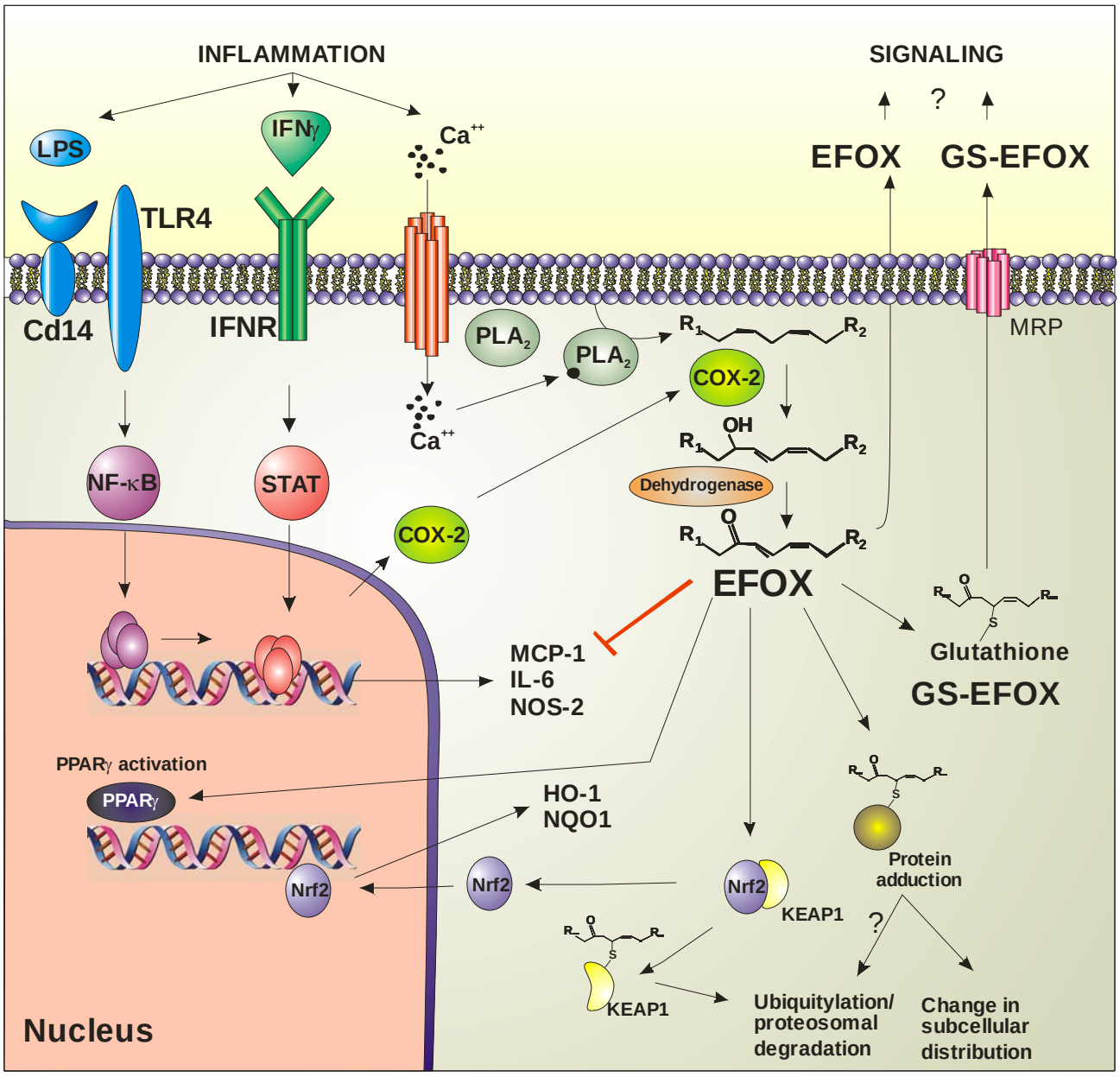


**Supplementary Fig. 1. EFOX generation, signaling and metabolism.** IFNγ and LPS can activate pro-inflammatory gene expression in macrophages via NF-κB and STAT signaling. Calcium influx also activates calcium-dependent $PLA_2$ thus releasing poly-unsaturated fatty acids from esterified lipids. Following inflammation-induced expression, COX-2 oxidizes poly-unsaturated fatty acids which are further converted to EFOXs by a constitutively active hydroxy-dehydrogenase. EFOX adducts of GSH are exported, while EFOX adduction to proteins may have effects on protein activity or subcellular localization. EFOXs can also modulate the transcription of pro-inflammatory genes and activate PPARγ and the Keap1/Nrf2 anti-oxidant response.

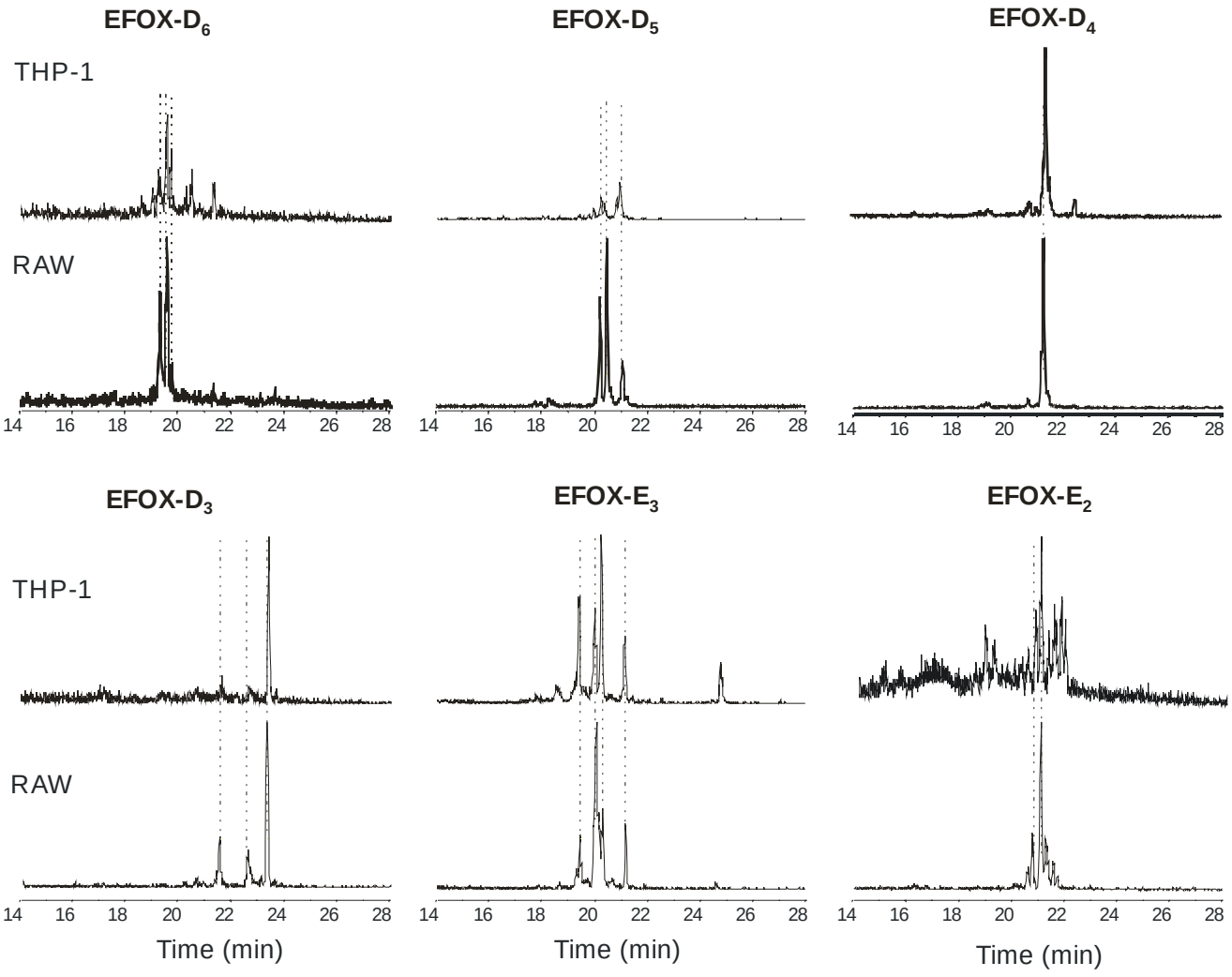


**Supplementary Fig. 2. EFOXs produced by THP-1 cells coelute with those produced by RAW264.7 cells.** THP-1 cells were differentiated with PMA (86 nM) for 16 h, activated with $Kdo_2$ (0.5 μg/ml) and IFNγ (200 U/ml), and EFOX levels were detected 8 h post activation. MRM scans following the neutral loss of 78 were used to detect EFOX-BME adducts.

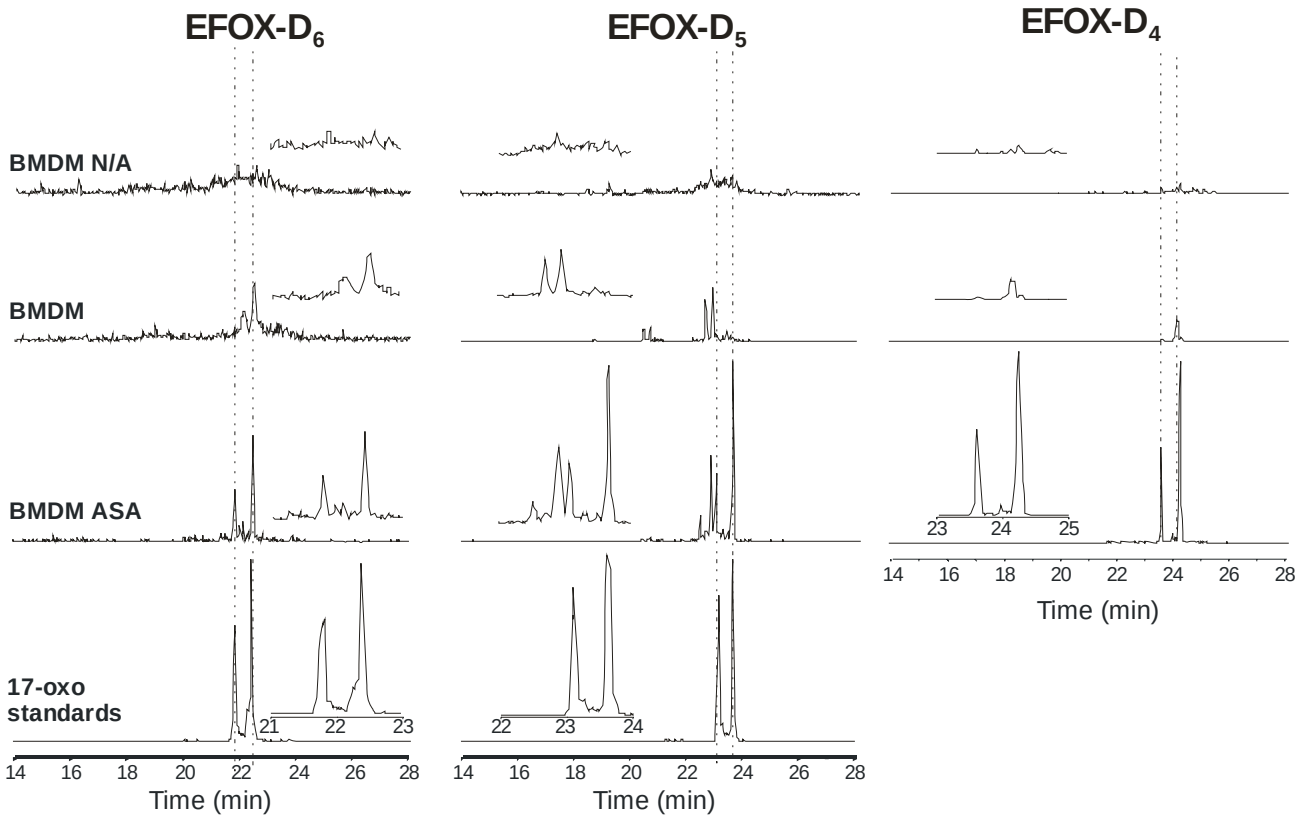


**Supplementary Fig. 3. EFOXs are formed in activated primary murine macrophages.** Bone marrow derived macrophages were activated with $Kdo_2$-(0.5 μg/ml) and IFNγ (200 U/ml) and EFOXs were detected 10 h post activation.

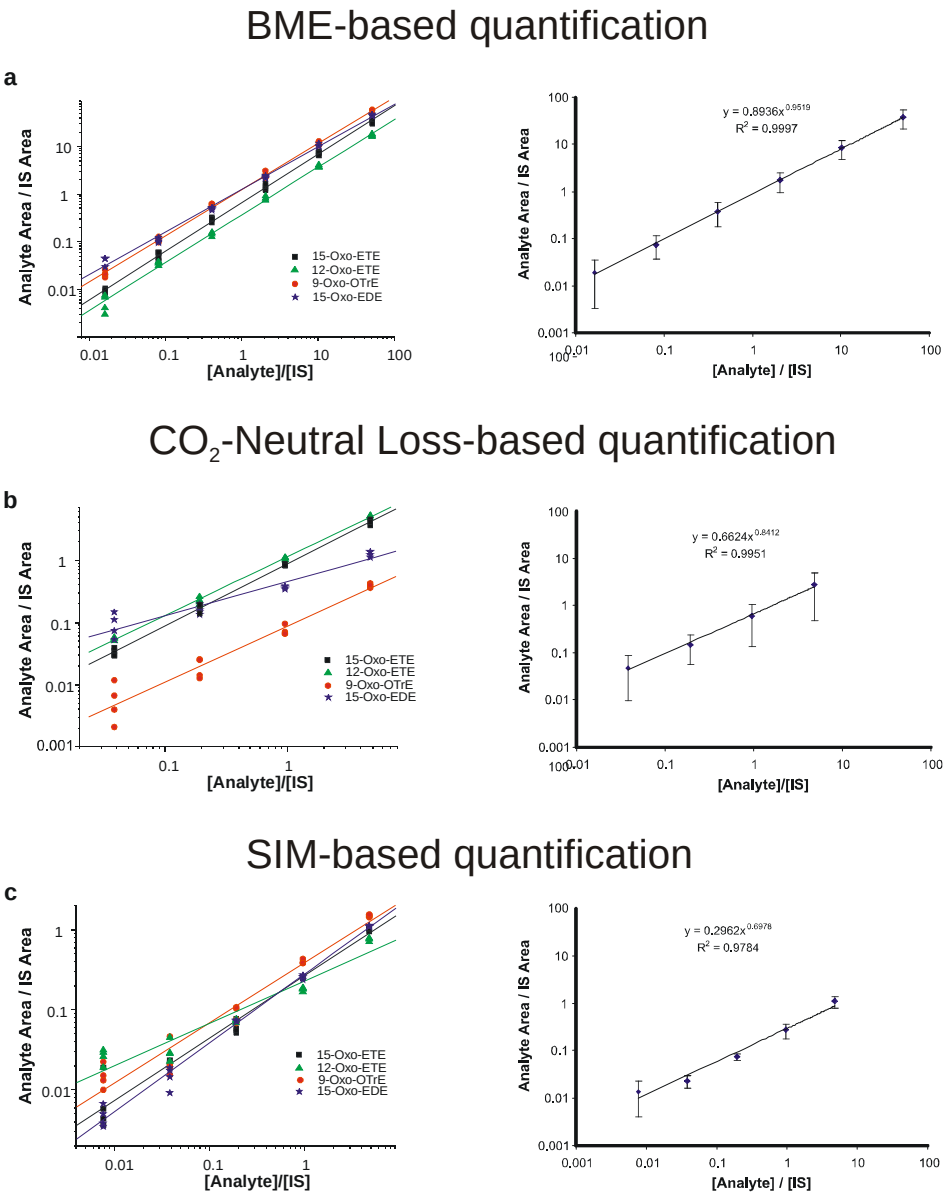


**Supplementary Fig. 4. BME adducts with α,β-unsaturated keto-derivatives yield the most reliable concentration curves for quantification by MS/MS.** (**a**) The compounds 15-OxoETE, 12-OxoETE, 15-OxoEDE and 9-OxoOTrE were reacted with BME for 2 h and concentration curves were prepared by serial dilution in the presence of 5-OxoETE-d7 as internal standard. (**b-c**) Serial dilution of 15-OxoETE, 12-OxoETE, 15-OxoEDE and 9-OxoOTrE were quantified by MRM in the presence of internal standard (5-oxoETE-d7) following the neutral loss of $CO_2$ (**b**) or by SIM (**c**), following parent mass. All peak areas corresponding to the compounds were normalized to the internal standard and plotted against their concentrations.

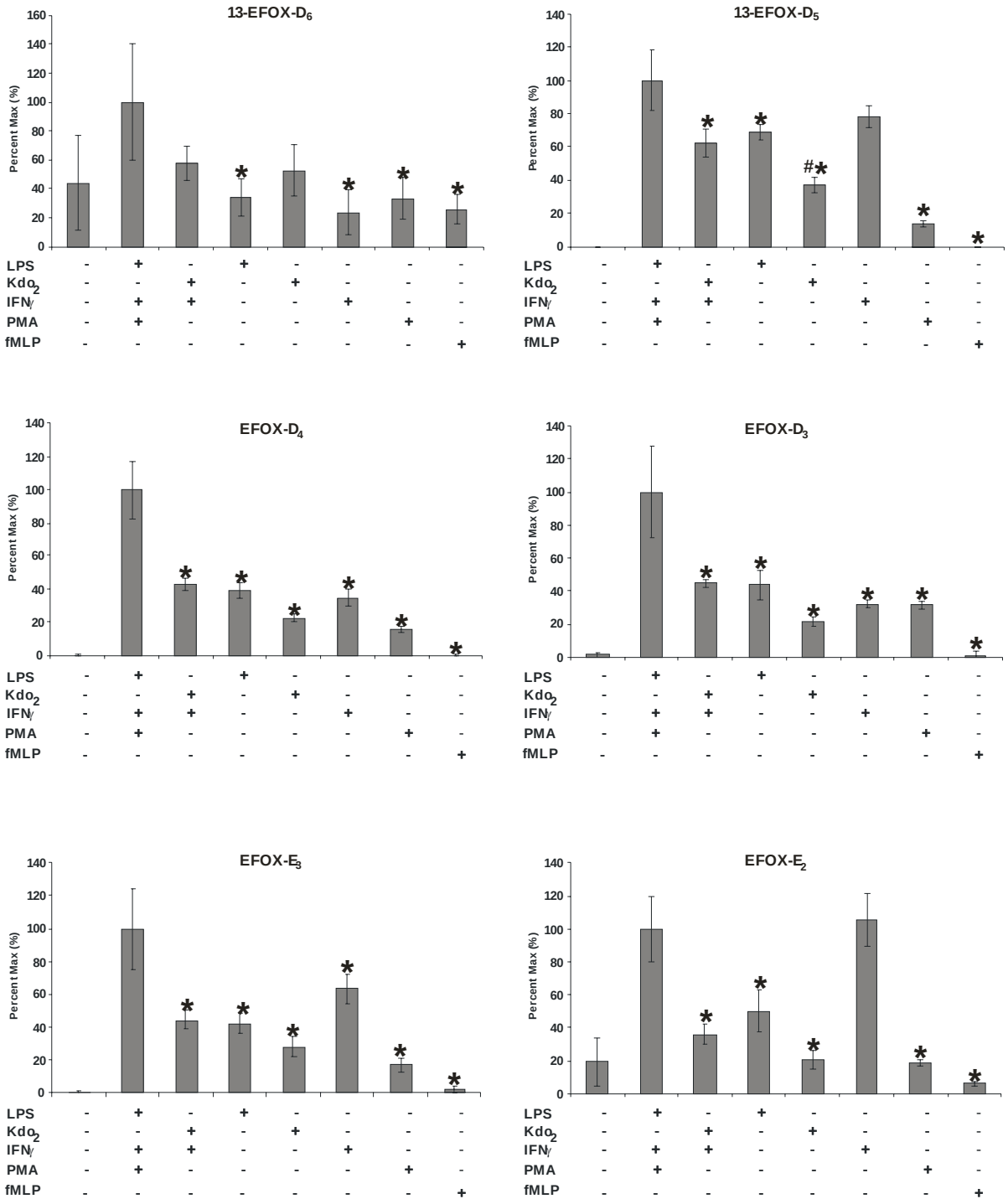


**Supplementary Fig. 5. EFOX production is dependent on RAW264.7 cell activation.** RAW264.7 cells were activated with the indicated compounds and EFOX levels were quantified 20 h post activation. Compound concentrations are as follows: LPS (0.5 μg/ml), $Kdo_2$ Lipid A (0.5 μg/ml), IFNγ (200 U/ml), PMA (3.24 μM), and fMLP (1 μM). Data are expressed as mean ± S.D. (n=4), where * = significantly different ($p$<0.01) from "PMA + IFNγ + LPS" and # = a significant difference ($p$<0.01)between LPS and "$Kdo_2$ + IFNγ" (one way ANOVA, post-hoc Tukey's test).

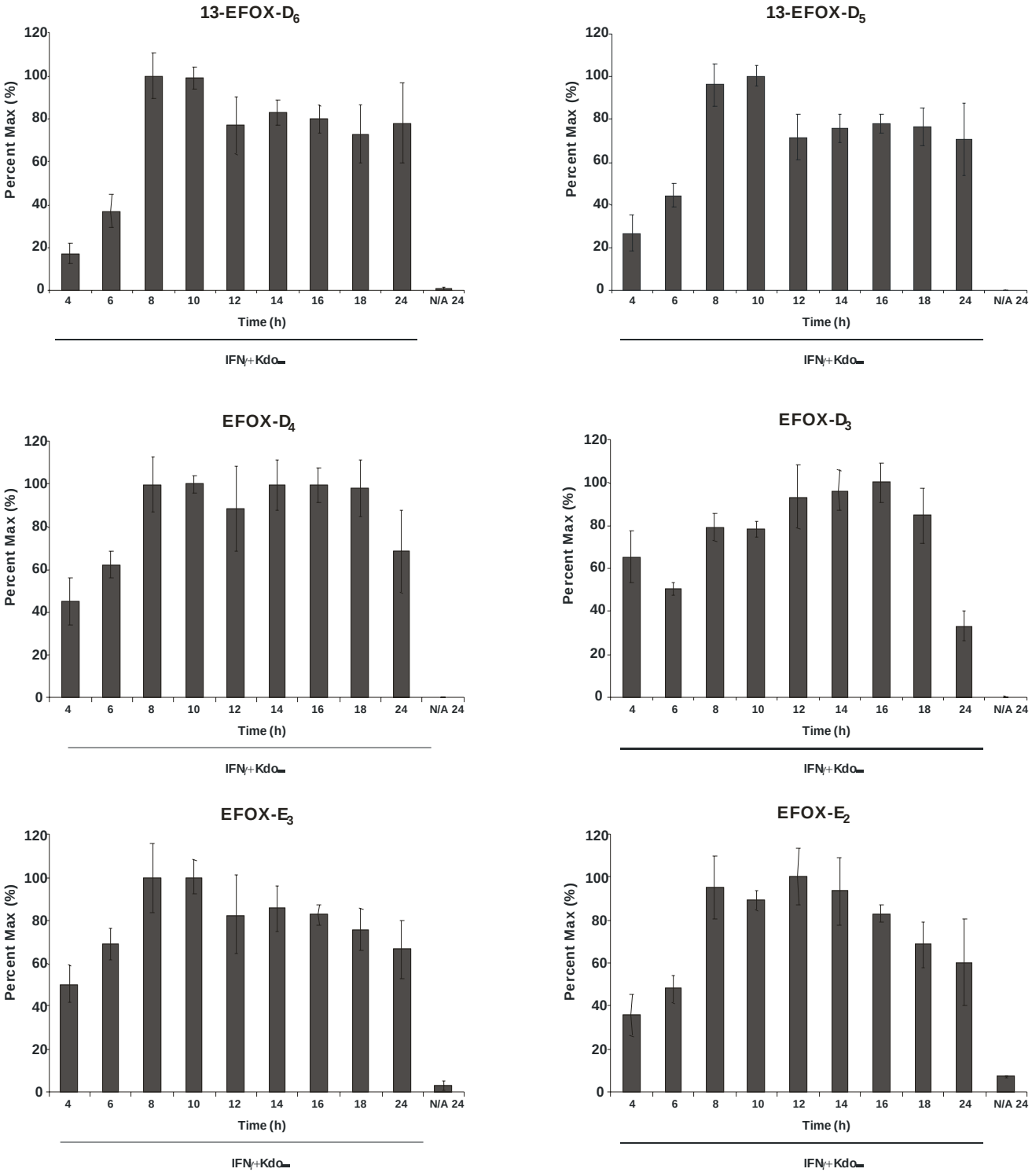


**Supplementary Fig. 6. EFOX production is time-dependent.** RAW264.7 cells were activated with $Kdo_2$ (0.5 μg/ml) and IFNγ (200 U/ml) and EFOX levels were quantified at indicated times post activation.

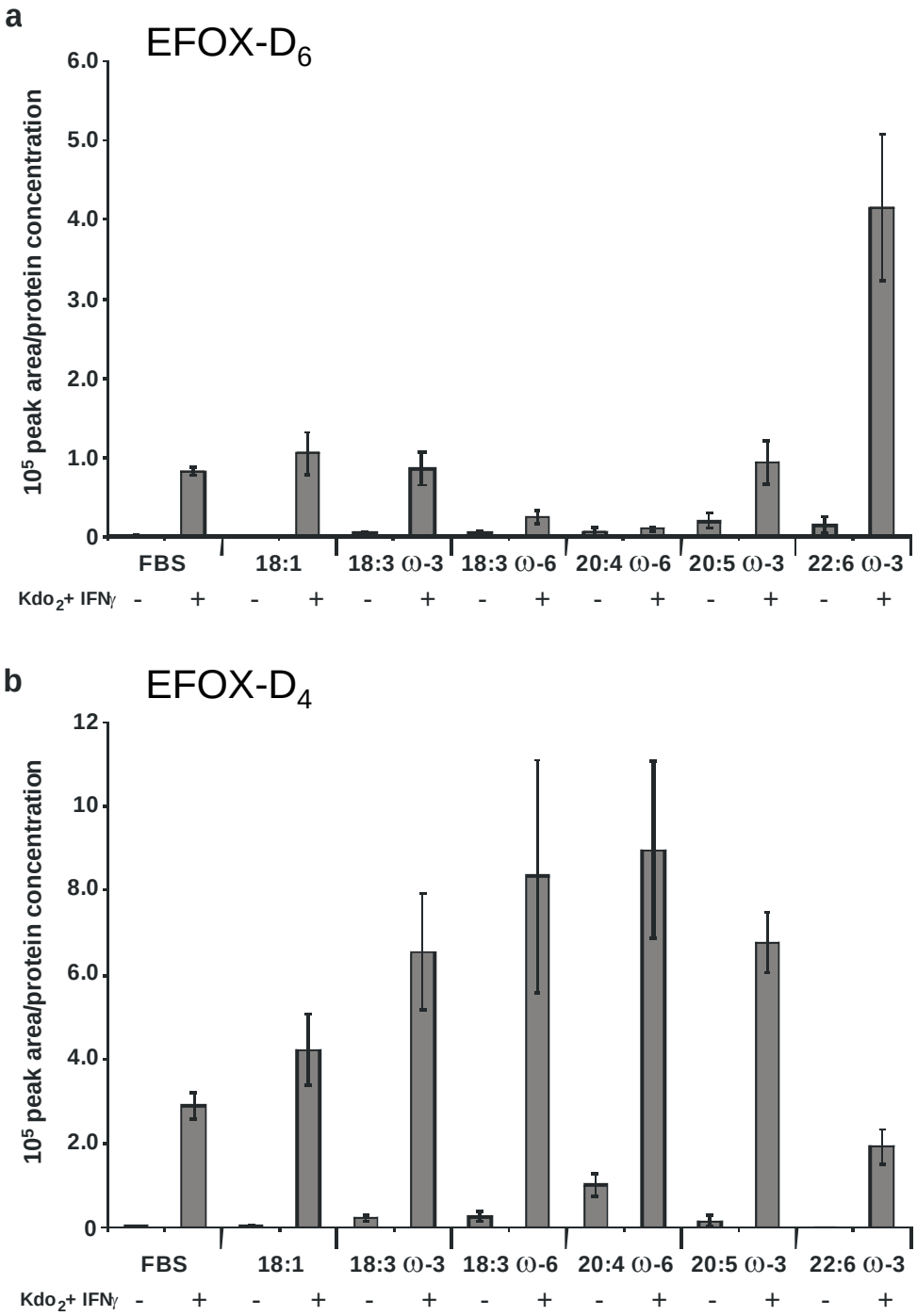


**Supplementary Fig. 7. 13-EFOX-$D_6$ and EFOX-$D_4$ are derived from the ω-3 series of fatty acids.** RAW264.7 cells were grown for 3 days in DMEM and 10% FBS supplemented with 32 μM of the indicated fatty acid. On the third day cells were activated with $Kdo_2$ 0.5 μg/ml) and IFNγ (200 U/ml) and 13-EFOX-$D_6$ and EFOX-$D_4$ levels were quantified 20 h post activation.

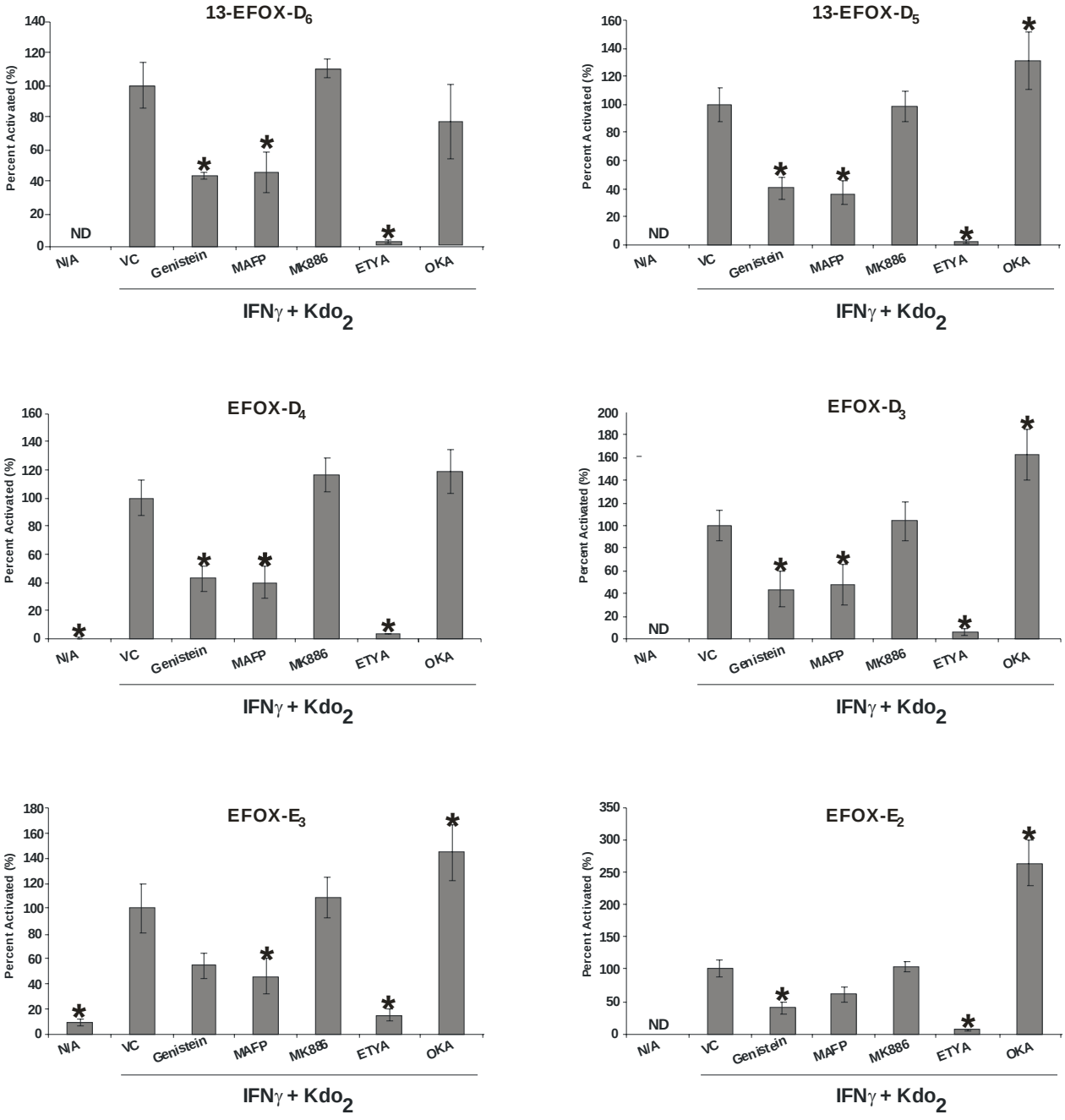


**Supplementary Fig. 8. EFOX formation is dependent on $PLA_2$ and COX-2 activity.** RAW264.7 cells were activated with $Kdo_2$ Lipid A (0.5 μg/ml) and IFNγ (200 U/ml) in the presence of the indicated inhibitors and 13-EFOX-$D_5$ levels were quantified 20 h post activation. Inhibitor concentrations were as follows: genistein (25 μM), MAFP (25 μM), MK886 (500 nM), ETYA (25 μM) and OKA (50 nM). Data are expressed as mean ± S.D. (n=4), where * = significantly different ($p$<0.01) from "$Kdo_2$ + IFNγ" (one-way ANOVA, post-hoc Tukey's test).

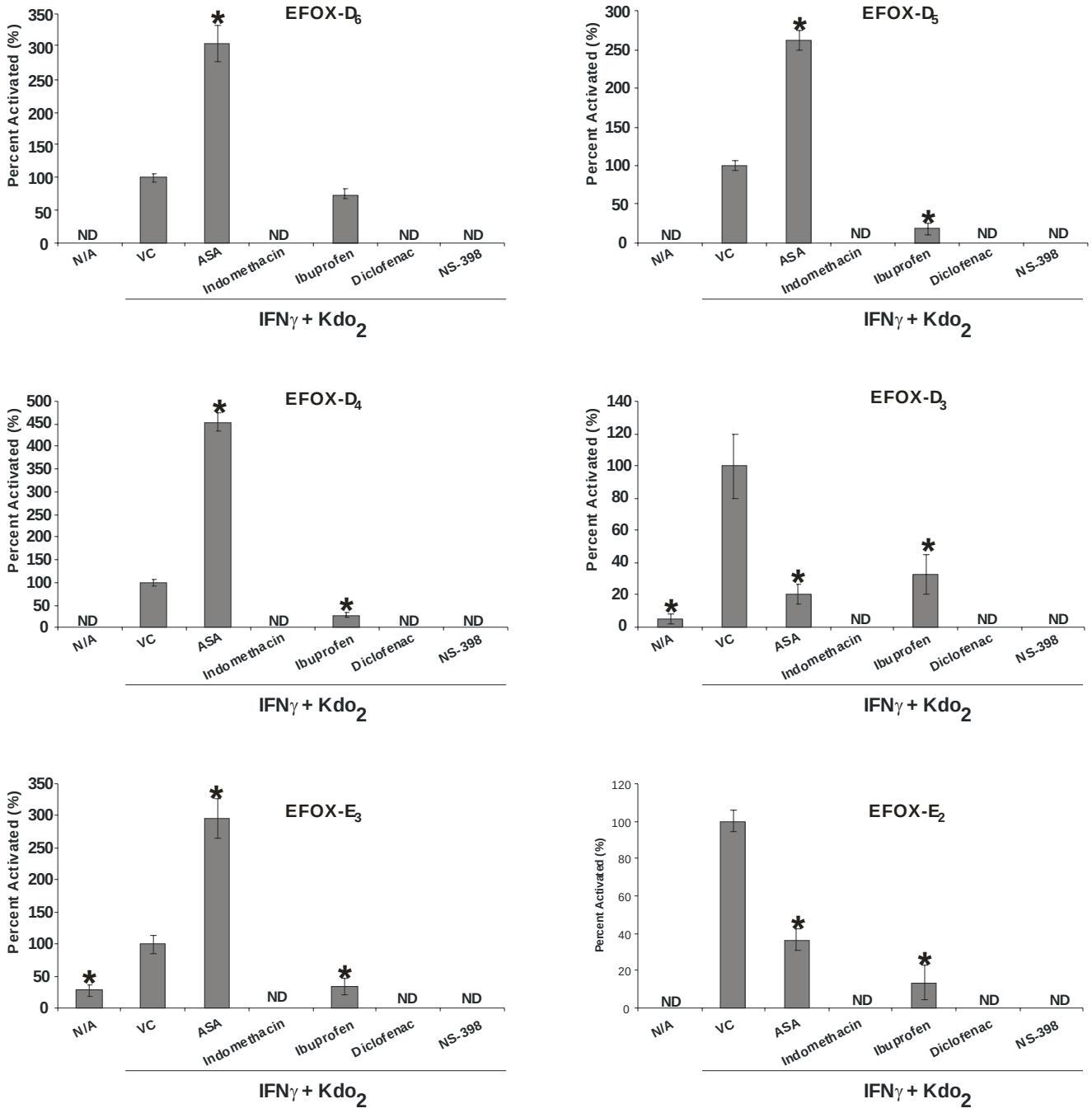


**Supplementary Fig. 9. EFOX formation is dependent on COX-2 activity.** RAW264.7 cells were activated with $Kdo_2$ (0.5 μg/ml) and IFNγ (200 U/ml) in the presence of indicated inhibitors and EFOX levels were quantified 20 h post activation. COX inhibitor concentrations were as follows: ASA (200 μM), indomethacin (25 μM), ibuprofen (100 μM), diclofenac (1 μM) and NS-398 (4 μM). Data are expressed as mean ± S.D. (n=4), where * = significantly different ($p$<0.01) from "$Kdo_2$ + IFNγ" (one way ANOVA, post-hoc Tukey's test).

a

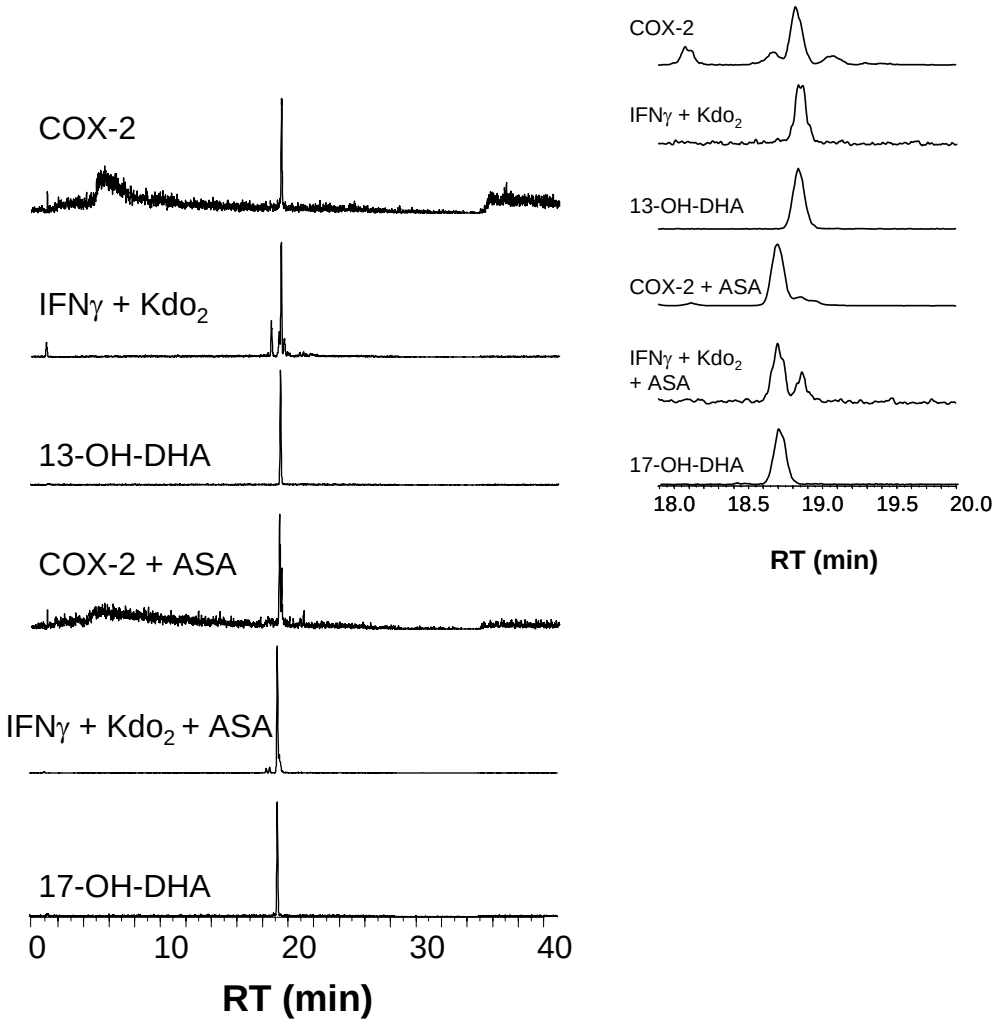


b

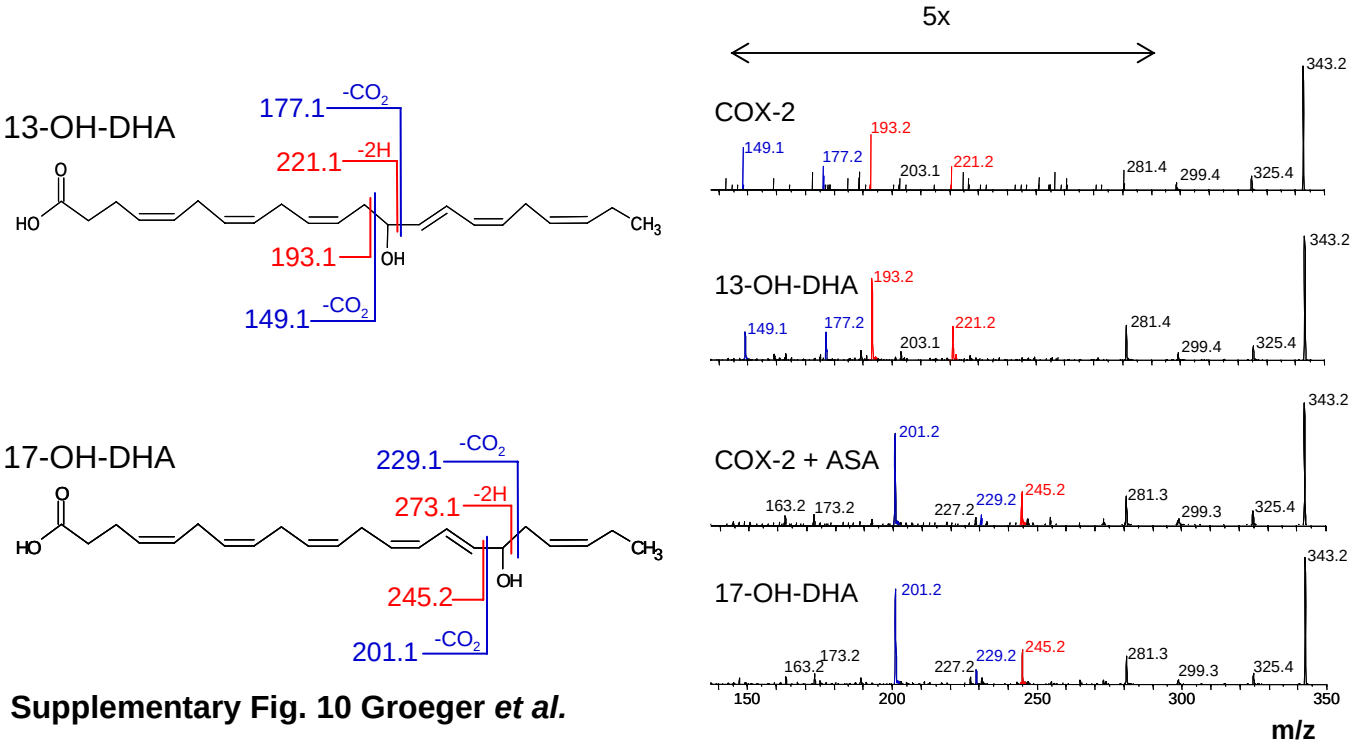


**Supplementary Fig. 10 Groeger *et al.***

C

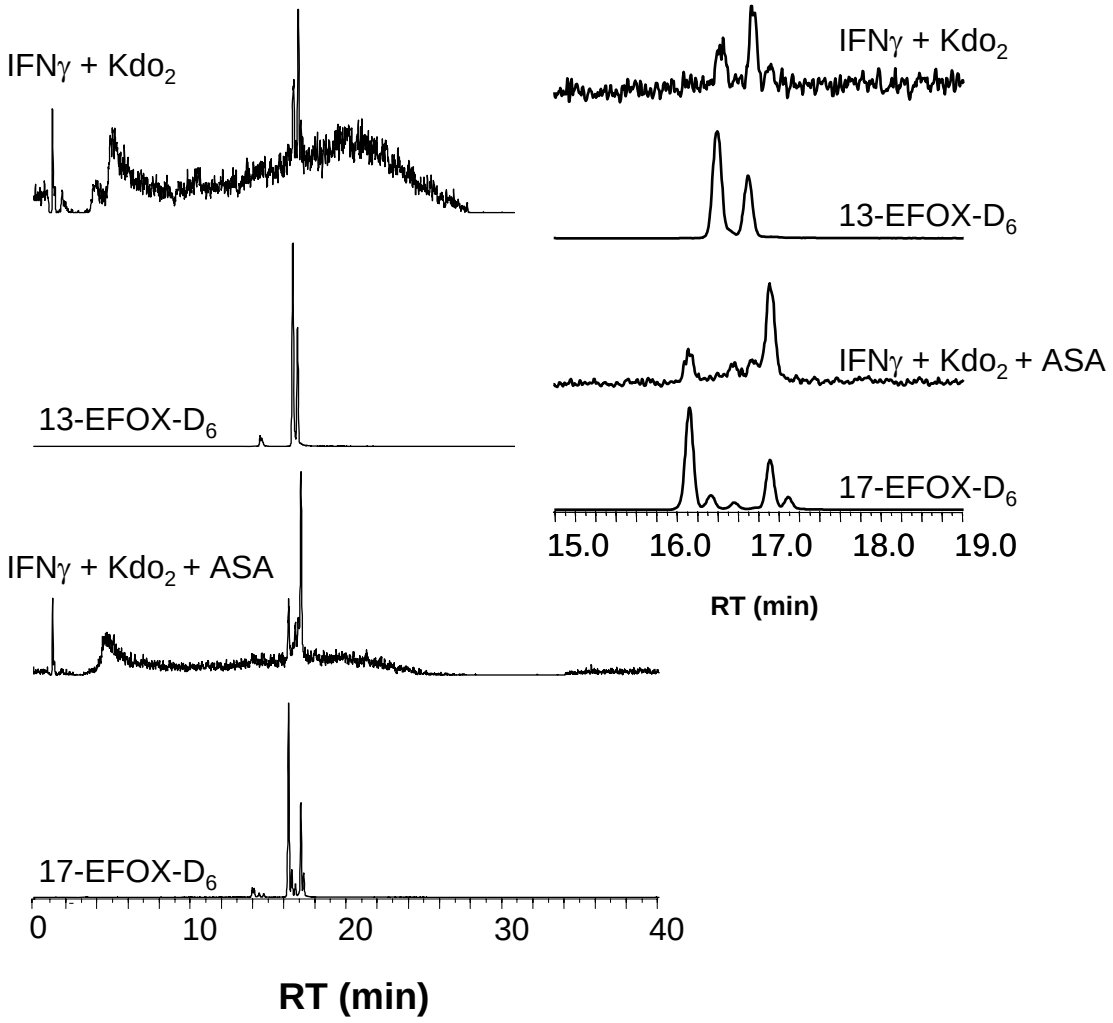


**Supplementary Figure 10. ASA-acetylated COX-2 produces 17-OH-DHA, rather than 13-OH-DHA, both *in vivo* and *in vitro*.** Chromatographic profiles (**a**) and mass spectra (**b**) of OH-DHA synthesized by COX-2 in presence of 10 μM DHA ±ASA. Chromatographic profiles of OH-DHA from cell lysates of activated RAW264.7 cells ($Kdo_2$ + IFNγ) ± ASA were also compared with 13-OH-DHA and 17-OH-DHA synthetic standards. **c**, Comparison of chromatographic profiles of EFOX-$D_6$ generated by activated RAW264.7 cells ($Kdo_2$ + IFNγ) ± ASA with 13-EFOX-$D_6$ and 17-EFOX-$D_6$ synthetic standards. The standards were enzymatically synthesized by incubating 20 μM 13- or 17-OH-DHA with 3α-hydroxysteroid dehydrogenase, in presence of 100μM $NAD^+$ for 10 min at 37°C. Enlarged chromatograms are reported in the insets.

a

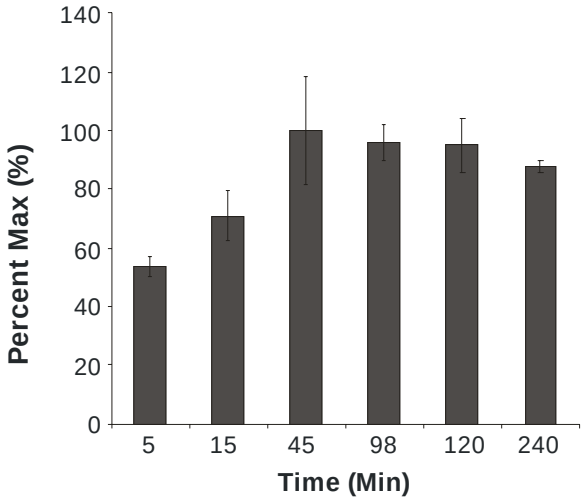


**Supplementary Fig. 11a Groeger *et al.***

b

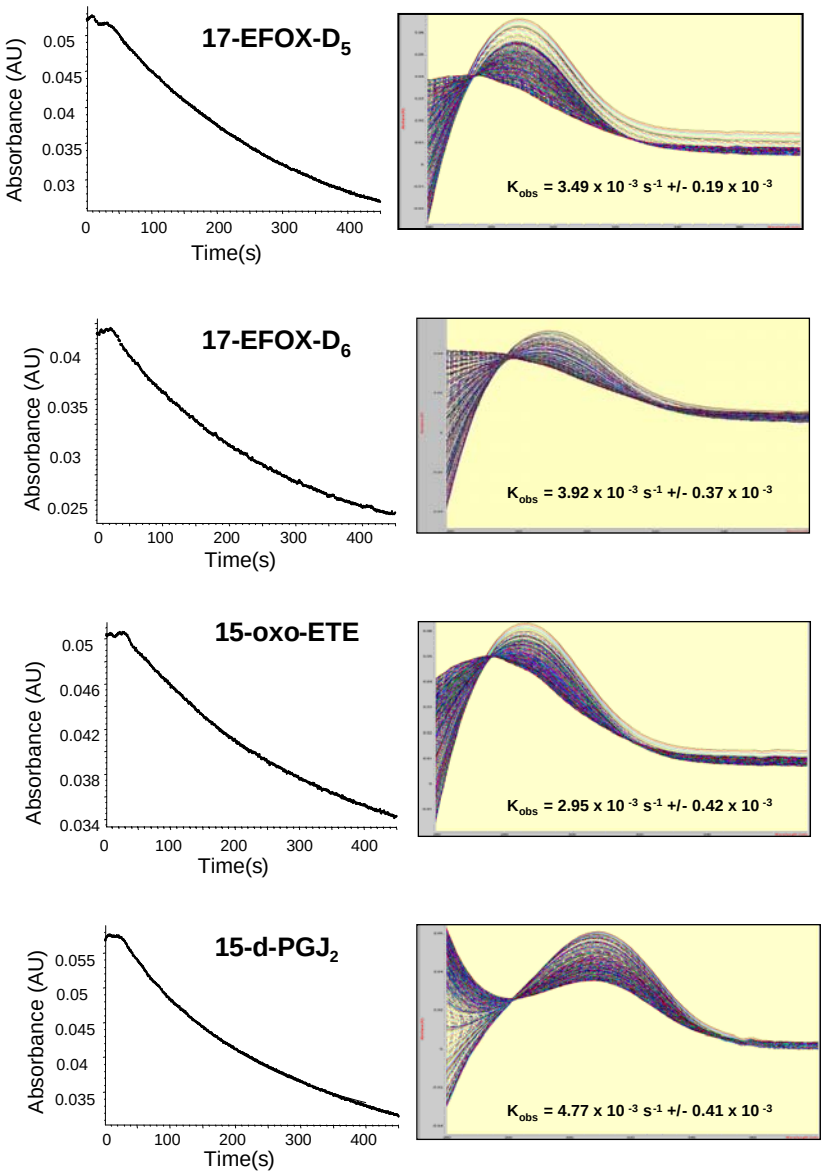


**Supplementary Fig. 11: EFOXs reactivity: a,** Time response of EFOX-$D_5$ reaction with activated RAW264.7 cell extracts. A fast reaction with free EFOX-$D_5$ was followed by a slower exchange of protein adducted EFOX-$D_5$. **b,** EOXs have a similar reactivity towards BME than other α,β-unsaturated carbonyl FA. The pseudo first order reaction rates between BME (50mM) and different α,β-unsaturated carbonyl FA (2.9 μM) were measured spectrophotometrically using a Agilent 8453 diode array as reported in **b.**

a

| Peptide 1 | | | | |
|---|---|---|---|---|
| | 17-EFOX-$D_5$-adducted | | non adducted | |
| aa | b | y | b | y |
| V | 100.08 | - | 100.08 | - |
| P | 197.13 | 1457.74 | 197.13 | 1745.02 |
| T | 298.18 | 1360.69 | 298.18 | 1647.97 |
| P | 395.23 | 1259.64 | 395.23 | 1546.92 |
| N | 509.27 | 1162.59 | 509.27 | 1449.87 |
| V | 608.34 | 1048.55 | 608.34 | 1335.82 |
| S | 695.37 | 949.48 | 695.37 | 1236.76 |
| V | 794.44 | 862.45 | 794.44 | 1149.72 |
| V | 893.51 | 763.38 | 893.51 | 1050.66 |
| D | 1008.54 | 664.31 | 1008.54 | 951.59 |
| L | 1121.62 | 549.28 | 1121.62 | 836.56 |
| T | 1222.67 | 436.2 | 1222.67 | 723.48 |
| C* (244) | 1382.7 | 335.15 | 1669.98 | 622.43 |
| R | - | 175.12 | - | 175.12 |

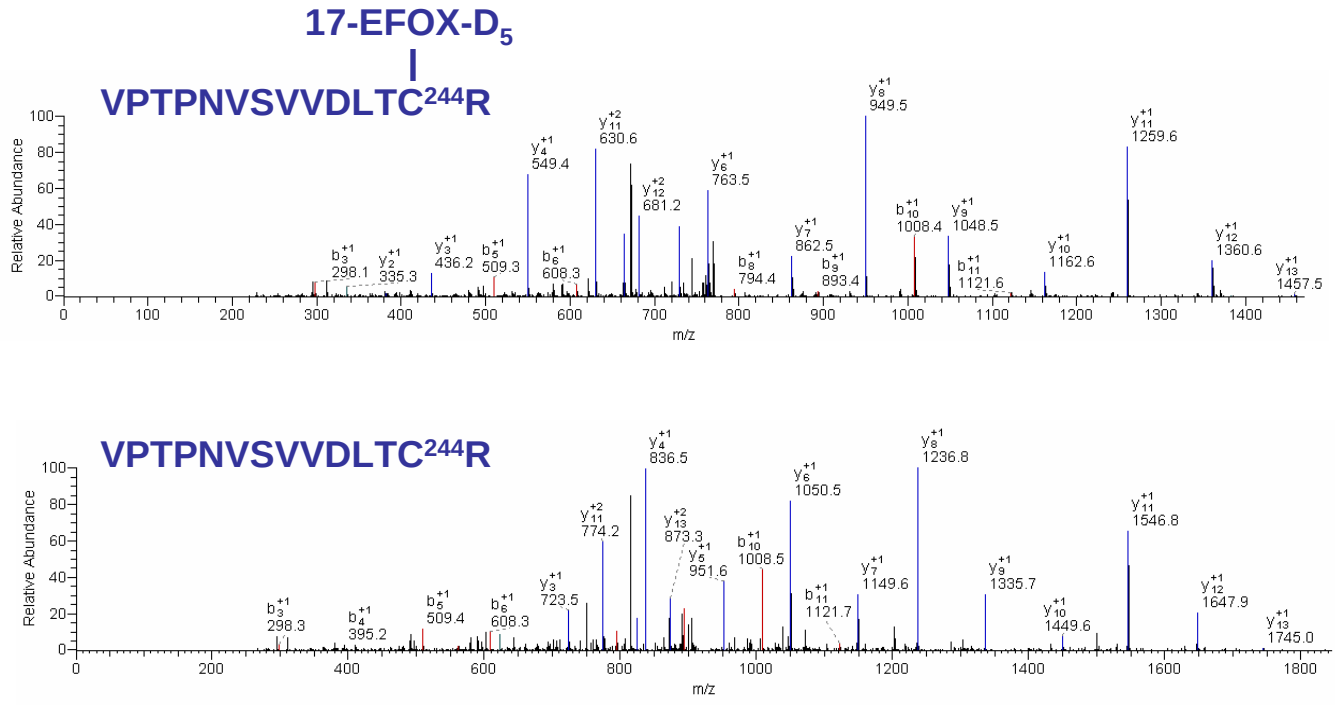


**Supplementary Fig. 12a Groeger *et al.***

b

| Peptide 2 | | | | |
|---|---|---|---|---|
| | 17-EFOX-$D_5$-adducted | | non adducted | |
| aa | b | y | b | y |
| V | 100.08 | - | 100.08 | - |
| I | 213.16 | 2863.61 | 213.16 | 2519.31 |
| H* | 694.52 | 2750.52 | 350.22 | 2406.22 |
| D | 809.55 | 2269.16 | 465.25 | 2269.16 |
| H | 946.60 | 2154.14 | 602.30 | 2154.14 |
| F | 1093.67 | 2017.08 | 749.37 | 2017.08 |
| G | 1150.69 | 1870.01 | 806.39 | 1870.01 |
| I | 1263.78 | 1812.99 | 919.48 | 1812.99 |
| V | 1362.85 | 1699.90 | 1018.55 | 1699.90 |
| E | 1491.89 | 1600.84 | 1147.59 | 1600.84 |
| G | 1548.91 | 1471.79 | 1204.61 | 1471.79 |
| L | 1661.99 | 1414.77 | 1317.69 | 1414.77 |
| M | 1793.04 | 1301.69 | 1448.74 | 1301.69 |
| T | 1894.08 | 1170.65 | 1549.78 | 1170.65 |
| T | 1995.13 | 1069.60 | 1650.83 | 1069.60 |
| V | 2094.20 | 968.55 | 1749.90 | 968.55 |
| H | 2231.26 | 869.48 | 1886.96 | 869.48 |
| A | 2302.30 | 732.43 | 1958.00 | 732.43 |
| I | 2415.38 | 661.39 | 2071.08 | 661.39 |
| T | 256.43 | 548.30 | 2172.13 | 548.30 |
| A | 2587.46 | 447.26 | 2243.16 | 447.26 |
| T | 2688.51 | 376.22 | 2344.21 | 376.22 |
| Q | 2816.57 | 275.17 | 2472.27 | 275.17 |
| K | | 147.11 | | 147.11 |

17-EFOX-$D_5$

VIHDHFGIVEGLMTTVHAITATQK

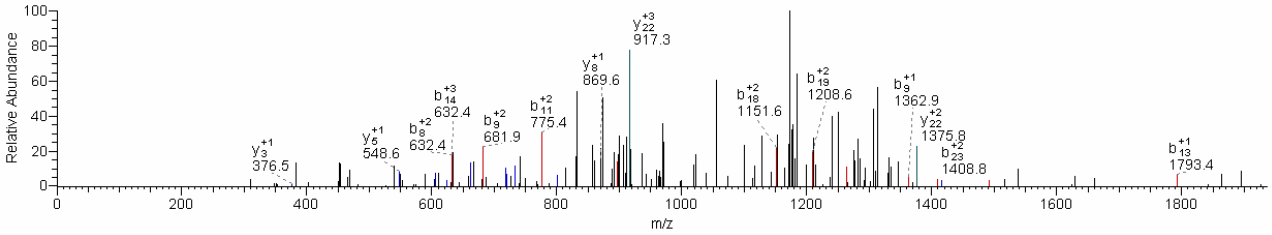


VIHDHFGIVEGLMTTVHAITATQK

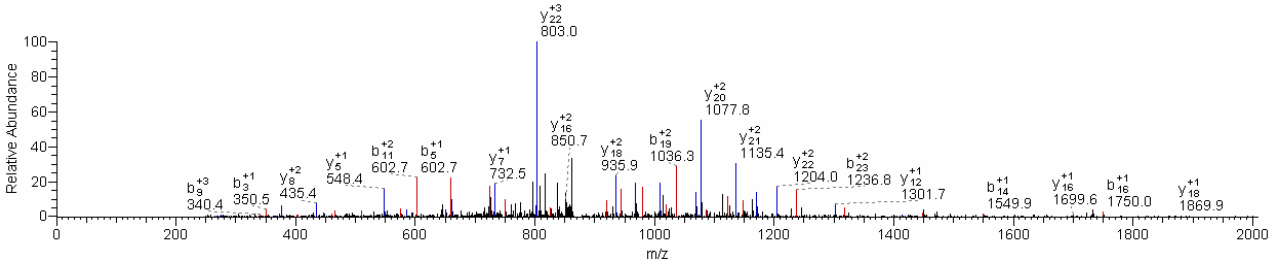


**Supplementary Fig. 12b Groeger *et al.***

C

| Peptide 3 | | | | |
|---|---|---|---|---|
| | 17-EFOX-$D_5$ -adducted | | non adducted | |
| aa | b | y | b | y |
| I | 114.09 | - | 114.09 | - |
| V | 213.60 | 1994.10 | 213.16 | 1706.82 |
| S | 300.19 | 1895.03 | 300.19 | 1607.75 |
| N | 414.23 | 1808.00 | 414.23 | 1520.72 |
| A | 485.27 | 1693.96 | 485.27 | 1406.68 |
| S | 572.30 | 1622.92 | 572.30 | 1335.64 |
| C# | 1019.61 | 1535.89 | 732.33 | 1248.61 |
| T | 1120.66 | 1088.58 | 833.38 | 1088.58 |
| T | 1221.71 | 987.53 | 934.43 | 987.53 |
| N | 1335.75 | 886.48 | 1048.47 | 886.48 |
| C* | 1495.78 | 772.44 | 1208.50 | 772.44 |
| L | 1608.87 | 612.41 | 1321.59 | 612.41 |
| A | 1679.90 | 499.32 | 1392.62 | 499.32 |
| P | 1776.96 | 428.29 | 1489.68 | 428.29 |
| L | 1890.04 | 331.23 | 1602.76 | 331.23 |
| A | 1961.08 | 218.15 | 1673.80 | 218.15 |
| K | - | 147.11 | - | 147.11 |

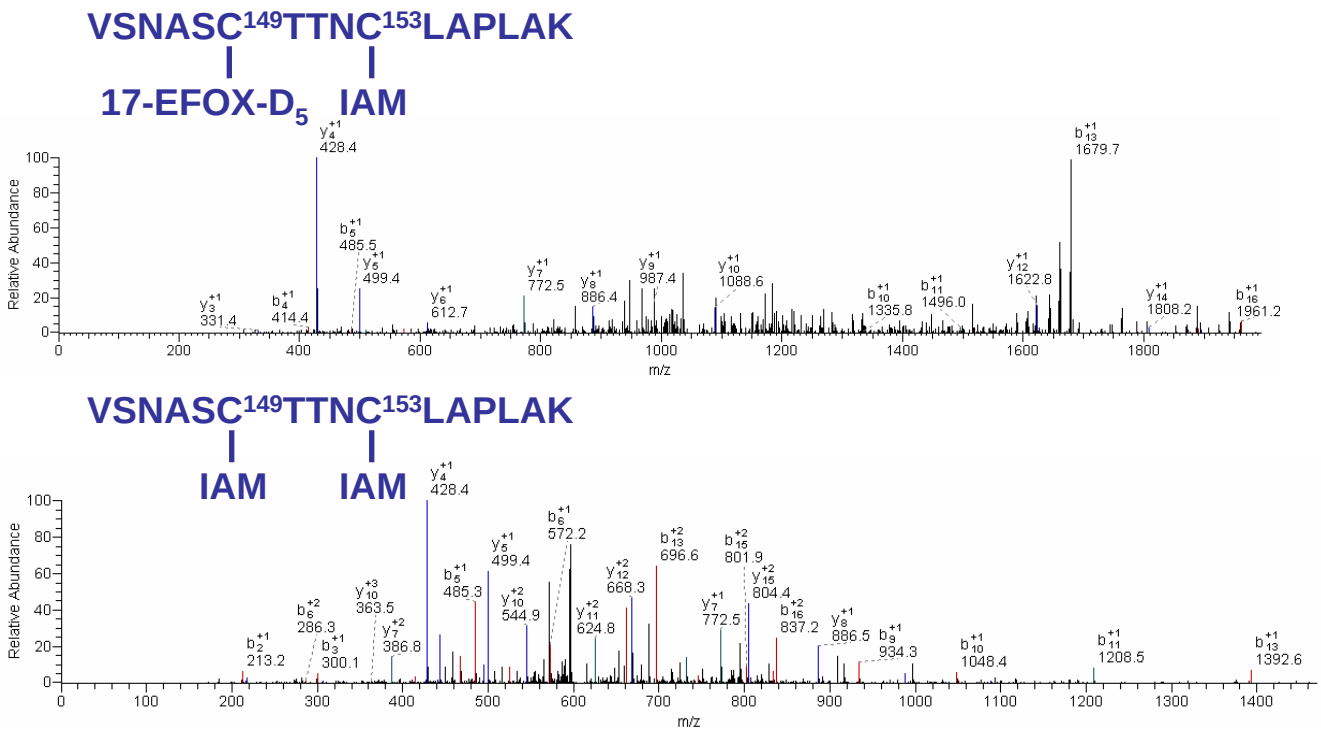


**Supplementary Fig. 12c Groeger *et al.***

d

| Peptide 4 | | | | |
|---|---|---|---|---|
| | 17-EFOX-$D_5$ -adducted | | non adducted | |
| aa | b | y | b | y |
| V | 100.80 | - | 100.80 | - |
| V | 199.14 | 1474.87 | 199.14 | 1130.57 |
| D | 314.17 | 1375.80 | 314.17 | 1031.50 |
| L | 427.26 | 1260.77 | 427.26 | 916.47 |
| M | 558.30 | 1147.69 | 558.30 | 803.39 |
| V | 657.36 | 1016.65 | 657.36 | 672.35 |
| H# | 1138.72 | 917.58 | 794.42 | 573.28 |
| M | 1269.76 | 436.22 | 925.46 | 436.22 |
| A | 1340.80 | 305.18 | 996.50 | 305.18 |
| S | 1427.83 | 234.14 | 1083.53 | 234.14 |
| K | - | 147.11 | - | 147.11 |

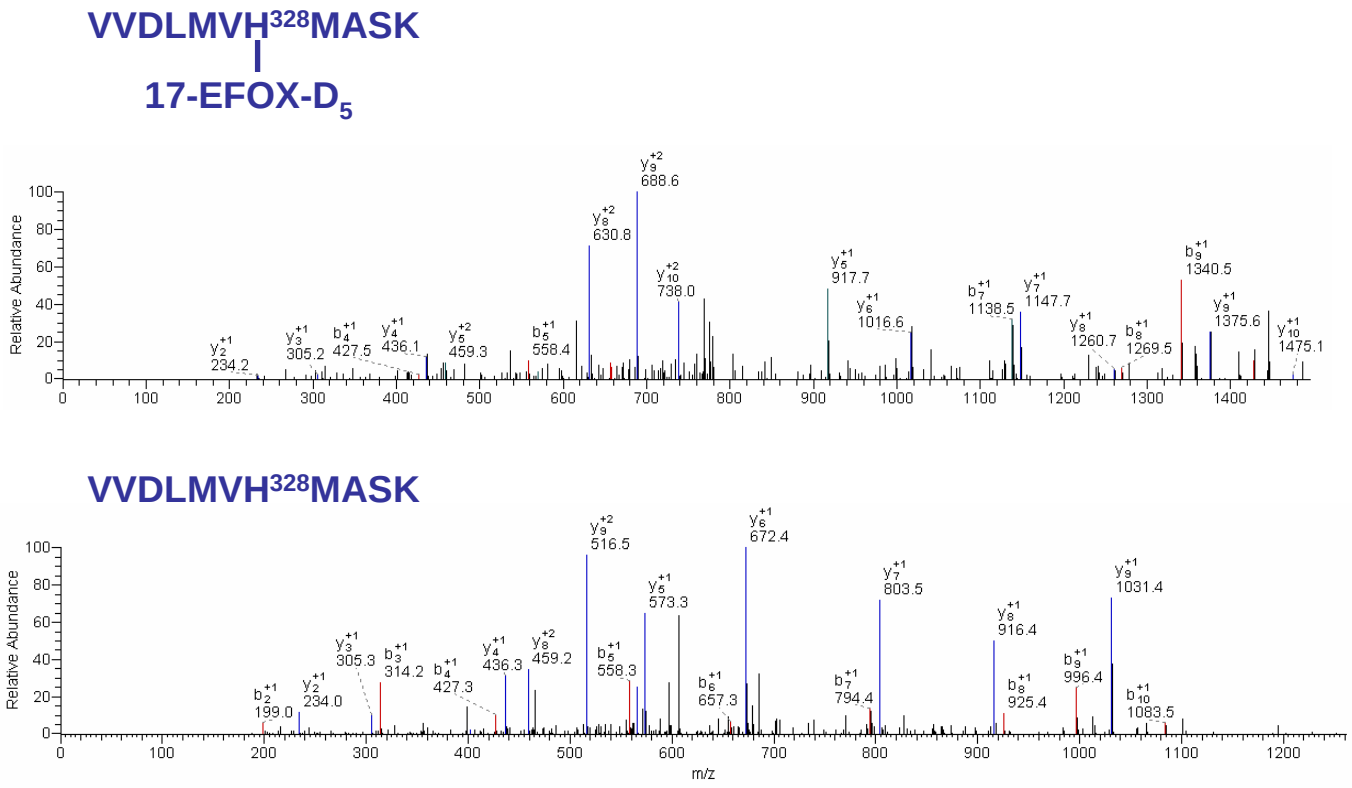


**Supplementary Fig. 12. Mass spectrometric analysis of *in vitro* reaction of GAPDH with 17-EFOX-$D_5$.** Four residues were detected and confirmed as being targets for 17-EFOX-$D_5$ in treated rabbit GAPDH. The peptides were alkylated at Cys 244 (**a**), His 163 (**b**), Cys 149 (**c**) and His 328 (**d**). Upper panels show 17-EFOX-$D_5$ modified peptides and lower panels show spectra from corresponding native peptide.

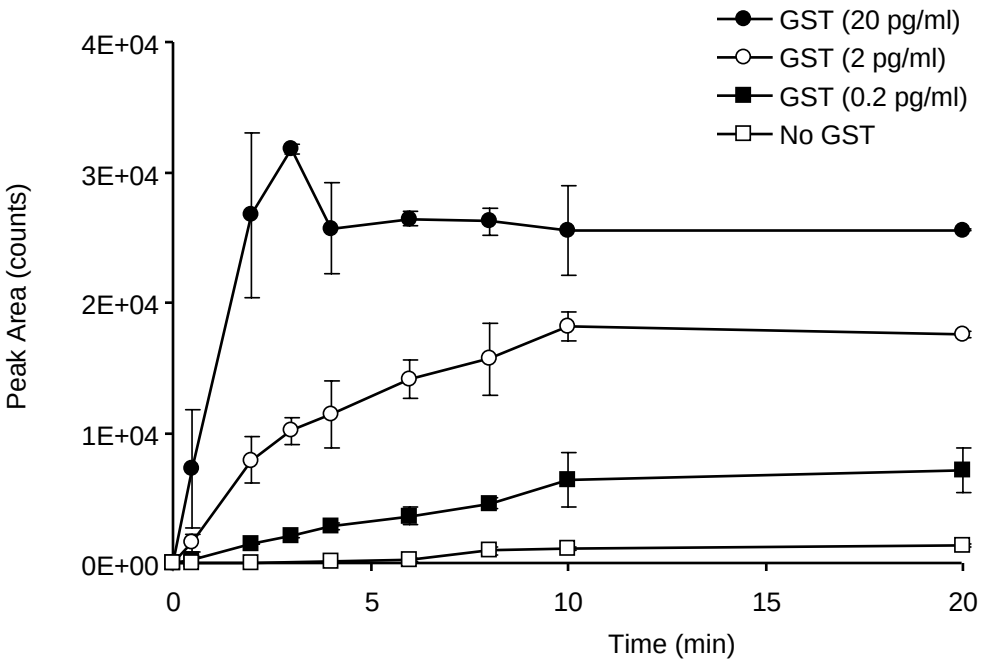


**Supplementary Fig. 13. 17-EFOX-$D_5$ is substrate of glutathione S-transferase (GST).** 17-EFOX-$D_5$ (20 μM) was incubated at 37° C in phosphate buffer at pH 8 with 0.1 mM glutathione and the indicated concentration of GST. Samples were collected at the indicated time points, excess GST was removed by acetonitrile precipitation followed by centrifugation. Formation of GS-17-EFOX-$D_5$ was monitored by nanoLC-MS/MS.

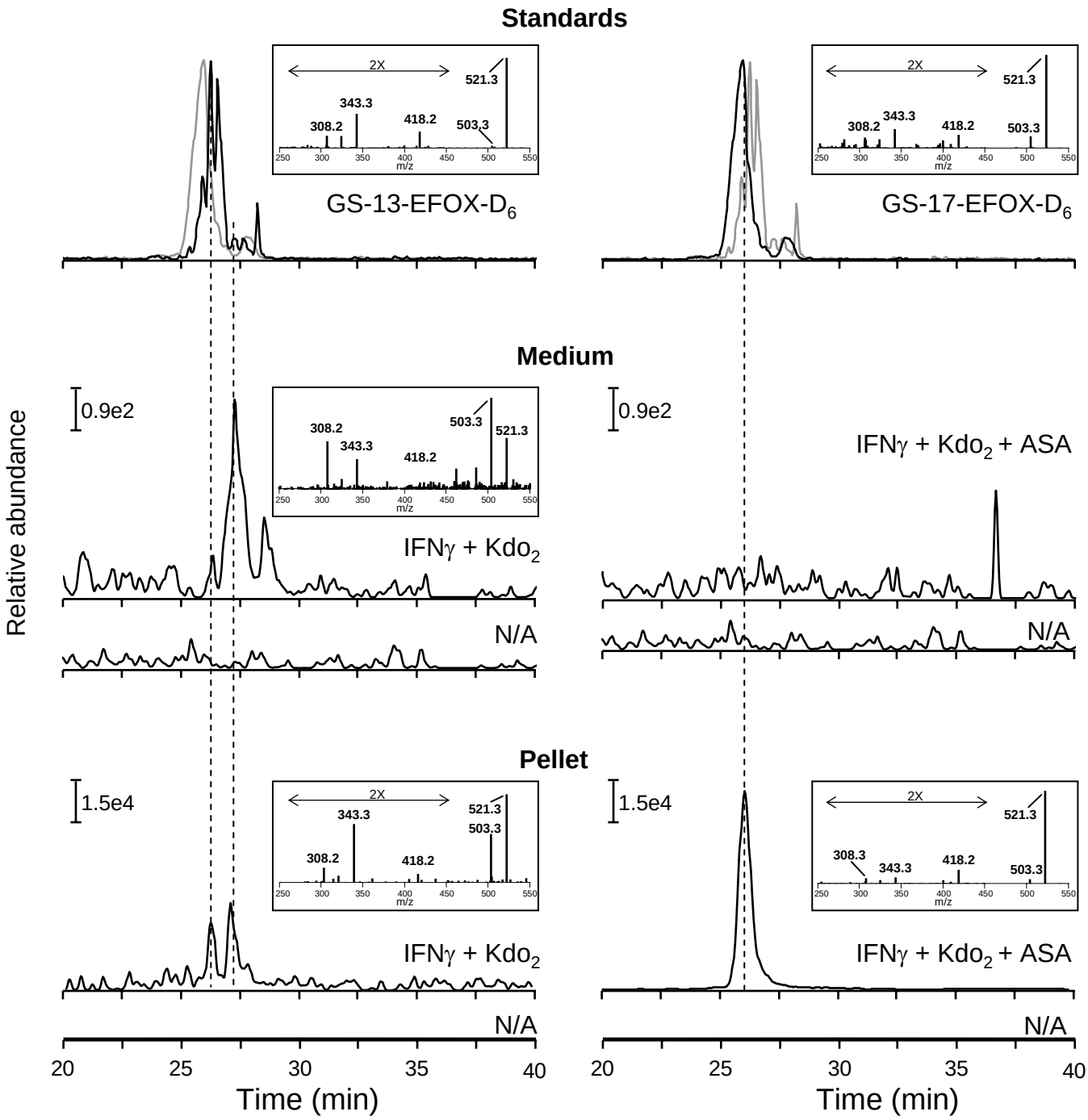


**Supplementary Fig. 14. Detection of GS-EFOX-$D_6$ adducts in pellets and media of activated RAW264.7 cells.** Chromatographic profiles and mass spectra of 13- and 17-EFOX-$D_6$ derived from synthesized standards (upper panels), cell medium (middle panel) and cell pellet (lower panel). Differences due to recovery efficiency were taken into account by correcting the signal levels using the internal standard GS-5-oxoETE-d7. Fragments 343.3 and 521.3 were selected and monitored as the ones giving the best signal to noise ratio in samples derived from cell media and cell pellets, respectively. Fragments 521.3 and 418.2 corresponded to fragments *y2* and *c1* while 343.3 and 308.2 derived from the lipid and the glutathione molecule. m/z 503.3 derived from loss of $H_2O$ from 523.3.

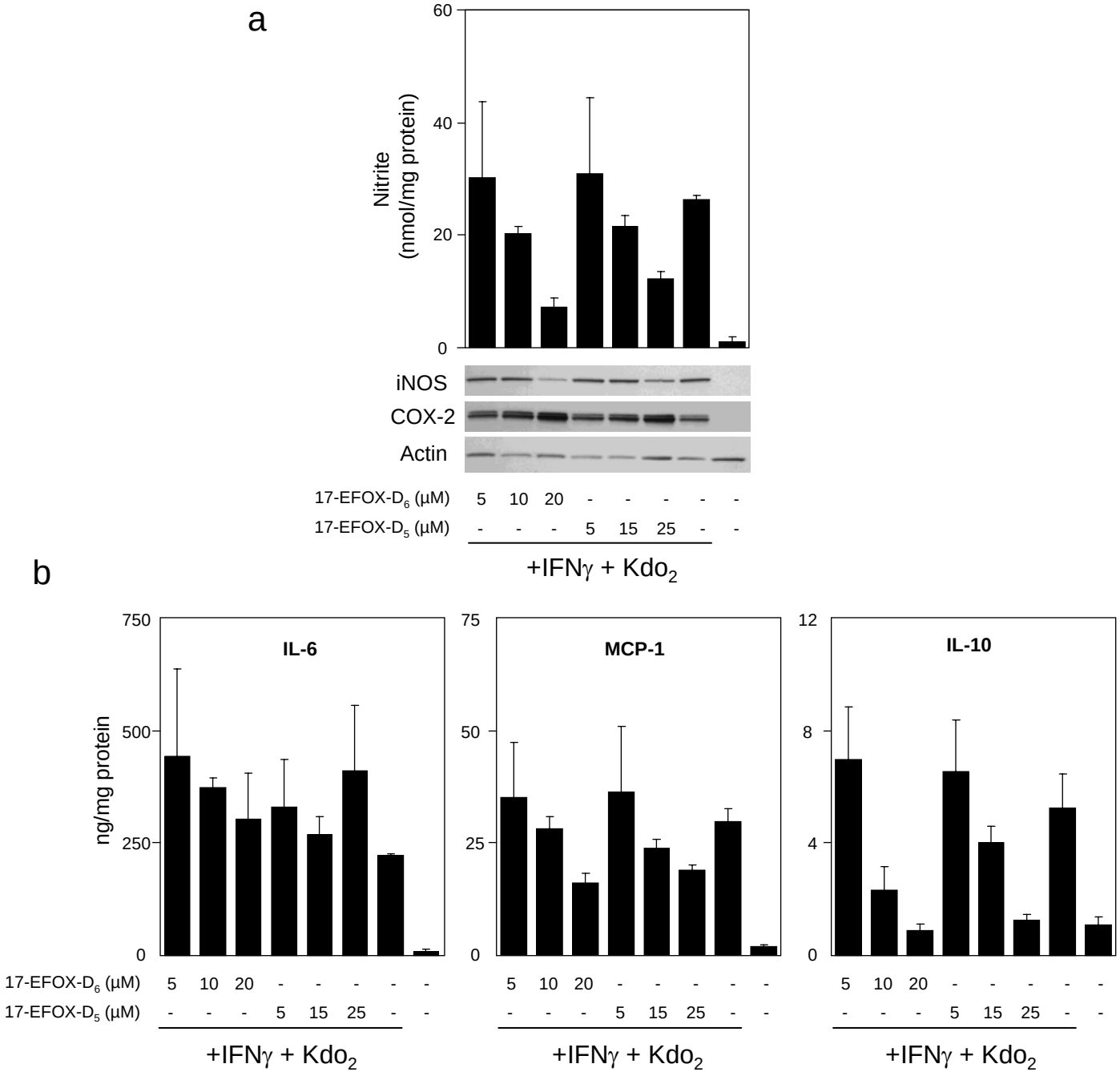


**Supplementary Fig. 15. 17-EFOX-D$_6$ and 17-EFOX-D$_5$ modulate the inflammatory response in bone marrow-derived macrophages.** Cells were treated with increasing concentration of 17-EFOX-D$_6$ and 17-EFOX-D$_5$ for 6h and Kdo$_2$ and IFNγ were added. Samples were collected at 12 h. **a**, Nitrite levels were measured in the cell media and normalized by the total protein content; iNOS and Cox-2 levels were measured in total cell lysates. **B**, IL-6, MCP-1 and IL-10 levels were measured in cell media and normalized by the total protein content.